J|A|C|S COMMUNICATIONS

Published on Web 08/30/2010

Nanostructured Gold Architectures Formed through High Pressure-Driven Sintering of Spherical Nanoparticle Arrays

Huimeng Wu,[†] Feng Bai,[‡] Zaicheng Sun,[‡] Raid E. Haddad,[‡] Daniel M. Boye,[§] Zhongwu Wang,[||] Jian Yu Huang,[†] and Hongyou Fan*[,†,‡]

Sandia National Laboratories, Advanced Materials Lab, 1001 University Boulevard SE, Albuquerque, New Mexico 87106, The University of New Mexico/NSF Center for Micro-Engineered Materials, Albuquerque, New Mexico 87131, Physics Department, Davidson College, Davidson, North Carolina 28035, and Cornell High Energy Synchrotron Source, Wilson Laboratory, Cornell University, Ithaca, New York 14853

Received June 23, 2010; E-mail: hfan@sandia.gov

Abstract: We have demonstrated pressure-directed assembly for preparation of a new class of chemically and mechanically stable gold nanostructures through high pressure-driven sintering of nanoparticle assemblies at room temperature. We show that under a hydrostatic pressure field, the unit cell dimension of a 3D ordered nanoparticle array can be reversibly manipulated allowing fine-tuning of the interparticle separation distance. In addition, 3D nanostructured gold architecture can be formed through high pressure-induced nanoparticle sintering. This work opens a new pathway for engineering and fabrication of different metal nanostructured architectures.

Nanostructured metal architectures exhibit important capabilities for catalytic,[1] sensor,[2] and fuel cell technologies.[3] The ability to control an interconnected metal framework over the nanometer scale is essential for these applications. "Dealloying" is one of several effective methods to fabricate 3D continuous metal nanostructures.[4] Through chemical reaction or thermal melting processes, the most electrochemically active elements are selectively removed leaving nanostructured metal architectures with disordered porosity.[5] This method generally requires lengthy, aggressive chemical reactions; high temperatures; and toxic, corrosive processing. A mild "etching" process was developed using silver nanocubes as sacrificial templates to synthesize nanostructured hollow gold architectures.[6] Other methods include block copolymer-templated growth[7] and physical deposition on a patterned substrate.[8] Here we report a pressure-directed assembly (PDA) method to fabricate 3D ordered, interconnected, gold nanostructures through high pressure-induced sintering of spherical gold nanoparticle arrays at room temperature. The fabrication process is simple and clean without requiring complicated chemical reactions, thermal processing, or purification to remove reaction byproduct.

The fabrications start with a thin film of ordered gold nanoparticle[9] arrays (see experimental details in the Supporting Information). The ordered gold nanoparticle films were made by solvent evaporation during spin-coating or solution-casting on silicon wafers. A piece of the gold nanoparticle film ($\sim 150 \times 150\ \mu m^2$) was peeled from the substrate and loaded directly into a diamond anvil cell. Silicone oil was used as the pressure transmitting fluid. Several pieces of ruby grain were used for pressure calibration.[10]

In situ small-angle X-ray scattering (SAXS) was performed to characterize the gold nanoparticle assembly and formation of 3D gold nanostructured architectures during compression and release. Before compression, the SAXS pattern of the film indicates that the nanoparticle arrays have a standard face-centered cubic (*fcc*) lattice structure ($Fm\bar{3}m$) with the unit cell parameter $a_{fcc} = 10.1$ nm (Figure S1A). Scanning electron microscopy (SEM) further verifies that the gold nanoparticles are organized in a periodic, ordered mesostructure (Figure 1A). The interparticle distance of 7.1 nm measured in the SEM images, corresponding to the $a_{fcc}/\sqrt{2}$ in the *fcc* lattice structure of the gold film, is in good agreement with the result from the SAXS measurement. Fast-Fourier transformation (FFT) analyses show a hexagonal pattern (Figure 1A, inset), with a preferred orientation along the [111] direction. Figure 1B shows the resulting 3D gold nanostructures after the pressure is released from 12.4 GPa to ambient pressure (also see Figure S2).

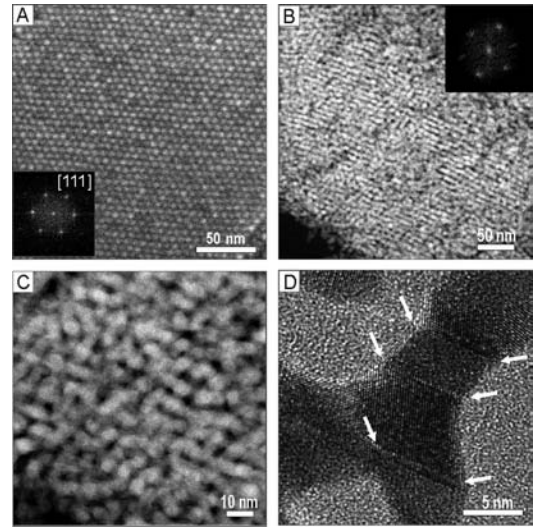

Figure 1. Structure of the ordered spherical gold nanoparticle films before and after compression. (A) A SEM image of a typical gold nanoparticle film before applying pressure. The inset is the FFT pattern of the film. (B) An STEM dark field image of 3D gold networks after releasing pressure from 12.4 GPa to ambient pressure. The diameter of the framework branches is 5.8 ± 0.5 nm. The inset is the FFT pattern of the networks. (C) An STEM image at higher magnification. (D) An HRTEM image of the gold networks. Individual crystal domains from the original spherical particles are connected together to form an interconnected network structure. Arrowheads point out twin boundaries.

In comparison with previous pressure works that focused only on individual nanoparticles,[11] several distinguished features are observed during the PDA process. First, the specimen remains ordered after compression up to ~12.4 GPa. The FFT pattern

[†] Sandia National Laboratories.
[‡] The University of New Mexico/NSF Center for Micro-Engineered Materials.
[§] Davidson College.
[||] Cornell University.

 10.1021/ja105255d

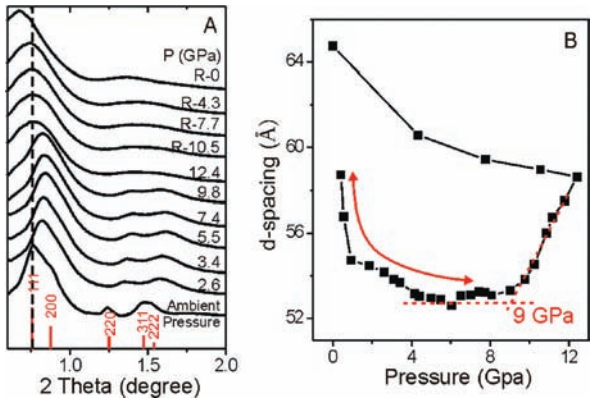

Figure 2. Structure evolution of gold nanoparticle arrays and formation of nanostructured gold architectures during compression and release. (A) HP-SAXS spectra integrated from HP-SAXS images of the nanoparticle film at varied pressures during compression and release (R−). (B) The *d*-spacing of the first Bragg reflection peak in the spectra (Figure 2A).

of the assembly (inset in Figure 1B) and SAXS (Figures 2A and S1B) confirm the ordered nature in the final gold network. Second, as shown in the scanning transmission electron microscopy (STEM) images (Figure 1B and 1C), the nanostructures are 3D interconnected. As a result, a nanoporous skeleton is formed with a pore size less than 5 nm; the compression process causes the diameter of gold skeleton (5.8 ± 0.5 nm) to become slightly larger than the diameter of the original spherical gold nanoparticles (5.1 ± 0.3 nm). Third, high resolution TEM imaging (Figure 1D) shows that twinning faults within an individual branched gold framework (or skeleton) are formed during the sintering of spherical nanoparticles, which confirms that the gold networks are formed by the multidirectional sintering of spherical gold nanoparticles.

The sintering of gold nanoparticles and the formation of 3D gold nanostructure were further examined by *in situ* high pressure small-angle X-ray scattering (HP-SAXS) studies. Figure 2A shows the compression−release sequence. Figure 2B shows the *d*-spacing of the first Bragg peak at varied pressures. When the pressure is less than ~9 GPa, the *fcc* mesostructure of the spherical nanoparticle assembly remains; the SAXS peaks shift to higher 2θ (lower *d*-spacing), which suggests that the compression causes the unit cell dimension of the particle assembly to shrink. For example, when pressure increases from ambient condition to 4.2 GPa, the *d*-spacing decreases from 5.9 to 5.1 nm. Further compressing to close to 9 GPa results in a minimal *d*-spacing before the particles contact and become sintered. When the pressure is released to ambient pressure, the *d*-spacing returns to 5.9 nm (Figure 2B), indicating the change of the unit cell dimension is reversible in the range of ambient pressure to 9 GPa (denoted by the bidirectional arrow in Figure 2B).

When the pressure is greater than 9 GPa, nanoparticle sintering occurs and an irreversible change of the unit cell dimension takes place. The *d*-spacing of the first Bragg peak increases rather than decreases with increasing pressure. This is probably due to the increase of the diameter of the gold framework (5.8 ± 0.5 nm) during the compression. Releasing the pressure from 12.4 GPa to ambient condition results in a larger *d*-spacing value (6.6 nm) than the starting one (5.9 nm), consistent with what has been observed by STEM studies (Figure 1B and 1C).

The formation of the 3D gold networks is driven by high pressure induced interparticle sintering. The gold nanoparticles are surface-stabilized by dodecanethiol monolayers. The organic monolayer essentially prevents nanoparticles from aggregation.

Scheme 1. Formation of 3D Nanostructured Gold Architecture via High Pressure-Driven Sintering of Spherical Nanoparticle Arrays

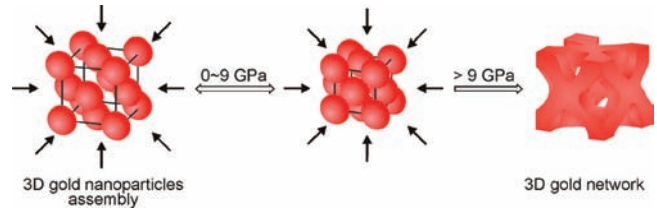

At ambient pressure, the nanoparticles within *fcc* arrays are stabilized by balancing the forces of interparticle attractions and van der Waal interactions due to alkane chain interdigitation. At lower pressure (<9 GPa), the nanoparticle arrays are compressed under a hydrostatic pressure field. The isotropic pressure applied uniformly through all directions to the nanoparticle assembly causes the *fcc* unit cell dimension to shrink uniformly. The overall pressure is not high enough to break the balanced forces[12] between adjacent nanoparticles. Hence the nanoparticle array maintained its *fcc* mesostructure and [111] orientation evidenced by SAXS results (Figure 2A). When pressure is high enough (>9 GPa), a nonhydrostatic pressure field across the sample is generated.[11c,13] This uniaxial pressure essentially overcomes the balanced forces[12] between adjacent nanoparticles and drives the nanoparticles to contact, to coalesce, and finally to sinter together. The pressure essentially does not affect the sintering orientation of the gold nanoparticles within {110} planes (Figure 2). In the *fcc* nanoparticle mesophase, the closest interparticle spacings are those within {110} planes. Consequently, these particles touch and sinter first, forming the skeleton. Ultimately, 3D ordered gold networks are formed (Scheme 1). During this process, partial dissociation of ligands at the contact points of the nanoparticle surface may occur.

In summary, the PDA method is a new and simple method for preparation of ordered chemically and mechanically stable gold nanostructures through mechanical compression of spherical nanoparticle arrays at room temperature. Through careful design of nanoparticle assembly and orientation, we expect different nanostructures can be accomplished.

Acknowledgment. This work was supported by the US DOE BES Program, Sandia National Laboratories' LDRD program, and NSF (DMI-0625897). STEM and TEM studies were performed in the Center of Integrated Nanotechnologies at the Sandia National Laboratories. CHESS is supported by the NSF and NIH/NIGMS via NSF Award DMR-0225180. Sandia is a multiprogram laboratory operated by Sandia Corporation, a Lockheed Martin Co., for the US DOE's National Nuclear Security Administration under Contract DE-AC04-94AL85000.

Supporting Information Available: Full experimental details and characterizations. This material is available free of charge via the Internet at http://pubs.acs.org.

References

(1) (a) Wittstock, A.; Zielasek, V.; Biener, J.; Friend, C. M.; Baumer, M. *Science* **2010**, *327*, 319–322. (b) Ding, Y.; Chen, M. W.; Erlebacher, J. *J. Am. Chem. Soc.* **2004**, *126*, 6876–6877. (c) Zielasek, V.; Jurgens, B.; Schulz, C.; Biener, J.; Biener, M. M.; Hamza, A. V.; Baumer, M. *Angew. Chem., Int. Ed.* **2006**, *45*, 8241–8244. (d) Xu, C. X.; Su, J. X.; Xu, X. H.; Liu, P. P.; Zhao, H. J.; Tian, F.; Ding, Y. *J. Am. Chem. Soc.* **2007**, *129*, 42–43.

(2) (a) Kucheyev, S. O.; Hayes, J. R.; Biener, J.; Huser, T.; Talley, C. E.; Hamza, A. V. *Appl. Phys. Lett.* **2006**, *89*, 053102. (b) Chen, L. Y.; Yu, J. S.; Fujita, T.; Chen, M. W. *Adv. Funct. Mater.* **2009**, *19*, 1221–1226. (c) Xiong, Y. J.; McLellan, J. M.; Chen, J. Y.; Yin, Y. D.; Li, Z. Y.; Xia, Y. N. *J. Am. Chem. Soc.* **2005**, *127*, 17118–17127.

(3) Lux, K. W.; Rodriguez, K. J. *Nano Lett.* **2006**, *6*, 288–295.
(4) (a) Erlebacher, J.; Aziz, M. J.; Karma, A.; Dimitrov, N.; Sieradzki, K. *Nature* **2001**, *410*, 450. (b) Sun, L.; Chien, C.-L.; Searson, P. C. *Chem. Mater.* **2004**, *16*, 3125.
(5) Li, R.; Sieradzki, K. *Phys. Rev. Lett.* **1992**, *68*, 1168.
(6) (a) Yavuz, M. S.; Cheng, Y. Y.; Chen, J. Y.; Cobley, C. M.; Zhang, Q.; Rycenga, M.; Xie, J. W.; Kim, C.; Song, K. H.; Schwartz, A. G.; Wang, L. H. V.; Xia, Y. N. *Nat. Mater.* **2009**, *8*, 935–939. (b) Chen, J. Y.; Wang, D. L.; Xi, J. F.; Au, L.; Siekkinen, A.; Warsen, A.; Li, Z. Y.; Zhang, H.; Xia, Y. N.; Li, X. D. *Nano Lett.* **2007**, *7*, 1318–1322.
(7) Ryu, J.-H.; Park, S.; Kim, B.; Klaikherd, A.; Russell, T. P.; Thayumanavan, S. *J. Am. Chem. Soc.* **2009**, *131*, 9870.
(8) Srikanth, S.; Eugenia, K.; Ji-Hyun, J.; Michael, E. M.; Hao, J.; Thimoty, J. B.; Edwin, L. T.; Vladimir, V. T. *Adv. Mater.* **2010**, *22*, 12–1369.
(9) Zheng, N.; Fan, J.; Stucky, G. D. *J. Am. Chem. Soc.* **2006**, *128*, 6550.
(10) Mao, H. K.; Xu, J.; Bell, P. M. *J. Geophys. Res.* **1986**, *91*, 4673.
(11) (a) Frenkel, J. *J. Phys.* **1945**, *9*, 385. (b) Gutmanas, E. Y. *Powder Metall. Int.* **1983**, *3*, 129. (c) Guo, Q. X.; Zhao, Y. S.; Mao, W. L.; Wang, Z. W.; Xiong, Y. J.; Xia, Y. N. *Nano Lett.* **2008**, *8*, 972.
(12) Grochala, W.; Hoffman, R.; Feng, J.; Ashcroft, N. W. *Angew. Chem., Int. Ed.* **2007**, *46*, 3620–3642.
(13) Wu, H.; Bai, F.; Sun, Z.; Haddad, R. E.; Boye, D. M.; Wang, Z.; Fan, H. *Angew. Chem., Int. Ed.* DOI: 10.1002/anie.201001581.

JA105255D